Proceedings of ICRC 2001: 1 © Copernicus Gesellschaft 2001

ICRC 2001

# Heavy component of primary particles around the knee observed with the Tibet burst detector and air shower array

**The Tibet AS$\gamma$ Collaboration**

**M. Amenomori[1], S. Ayabe[2], S.W. Cui[3], L.K. Ding[3], X.Y.Ding[4], C.F. Feng[5], Z.Y. Feng[6], Y. Fu[5], X.Y. Gao[7], Q.X. Geng[7], H.W. Guo[4], M. He[5], K. Hibino[8], N. Hotta[9], J. Huang[9], Q. Huang[6], A.X. Huo[3], K. Izu[10], H.Y. Jia[6], F. Kajino[11], K. Kasahara[12], Y. Katayose[13], K. Kawata[11], Labaciren[4], G.M. Le[14], J.Y. Li[5], H. Lu[3], S.L. Lu[3], G.X. Luo[3], X.R. Meng[4], J. Mu[7], M. Nishizawa[15], M. Ohnishi[10], I. Ohta[9], T. Ouchi[10], S. Ozawa[9], J.R. Ren[3], T. Saito[16], M. Sakata[11], T. Sasaki[8], M. Shibata[13], A. Shiomi[10], T. Shirai[8], H. Sugimoto[17], K. Taira[17], M. Takita[10], Y.H. Tan[3], N. Tateyama[8], S. Torii[8], H. Tsuchiya[10], S. Udo[2], T. Utsugi[2], C.R. Wang[5], H. Wang[3], X. Wang[5], X.W. Xu[3,10], L. Xu[5], X.C. Yang[7], Y. Yamamoto[11], Z.H. Ye[14], G.C. Yu[6], A.F. Yuan[4], T. Yuda[18], H.M. Zhang[3], J.L. Zhang[3], N.J. Zhang[5], X.Y. Zhang[5], Zhaxiciren[4], and Zhaxisangzhu[4]**

[1]Department of Physics, Hirosaki University, Hirosaki, Japan
[2]Department of Physics, Saitama University, Urawa, Japan
[3]Cosmic Ray and High Energy Astrophysics Laboratory, IHEP, CAS, Beijing, China
[4]Department of Mathematics and Physics, Tibet University, Lhasa, China
[5]Department of Physics, Shangdong University, Jinan, China
[6]Institute of Modern Physics, South West Jiaotong University, Chengdu, China
[7]Department of Physics, Yunnan University, Kunming, China
[8]Faculty of Engineering, Kanagawa University, Yokohama, Japan
[9]Faculty of Education, Utsunomiya University, Utsunomiya, Japan
[10]Institute for Cosmic Ray Research, University of Tokyo, Kashiwa, Japan
[11]Department of Physics, Konan University, Kobe, Japan
[12]Faculty of Systems Engineering, Shibaura Institute of Technology, Omiya, Japan
[13]Department of of Physics, Yokohama National University, Yokohama, Japan
[14]Center of Space Science and Application Research, CAS, Beijing, China
[15]National Institute for Informatics, Tokyo, Japan
[16]Tokyo Metropolitan College of Aeronautical Engineering, Tokyo, Japan
[17]Shonan Institute of Technology, Fujisawa, Japan
[18]Solar-Terrestrial Environment Laboratory, Nagoya University, Nagoya Japan

**Abstract.** A hybrid experiment of the emulsion chamber, burst detector and air-shower array was done at Yangbajing (4300 m above sea level) in Tibet. From this experiment, we observed about 4300 burst events accompanied by air showers in excess of about $10^{14}$ eV during 690 days of operation. Out of these events, we further sorted out 11 events as those induced by heavy primaries ($H$, $VH$, and Fe) with its primary energy above about $10^{16}$ eV, using an artificial neural network. From this data, we obtained the absolute flux of heavy component at energies around several times $10^{16}$ eV. Our result suggests that heavy nuclei are the main component of the primary cosmic rays in the energy region around and beyond the knee.

## 1 Introduction

The energy spectrum of observed cosmic rays is expressed by a power law from about $10^{11}$ to $10^{20}$ eV with a slight change of slopes between $10^{15}$ eV and $10^{16}$ eV. The break of the all-particle spectrum at around several times $10^{15}$ eV is called the " knee". Although existence of the knee has well been confirmed experimentally, there are many arguments about explanation of the origin. Most cosmic rays in the Galaxy are produced by supernova explosion, and it is generally considered to be accelerated to about $10^{14}$ eV by the blast wave then generated. The acceleration model by supernova blast waves and a plausible propagation model of cosmic rays in the Galaxy can well explain a steeper power-law spectrum observed, suggesting a rigidity-dependent bending for different cosmic ray composition. However, there is no consensus on the origin of cosmic rays in the energy region beyond the knee.

The primary composition around the knee region has been extensively studied with ground based EAS technique by measuring secondary electrons, muons, hadrons and Čerenkov light. However, the conclusions obtained on the mass composition sometimes differ with experiments considerably. Therefore, measurements of the primary cosmic rays around the knee are crucial to resolve knee puzzle.

*Correspondence to:* yuda (yuda@stelab.nagoya-u.ac.jp)

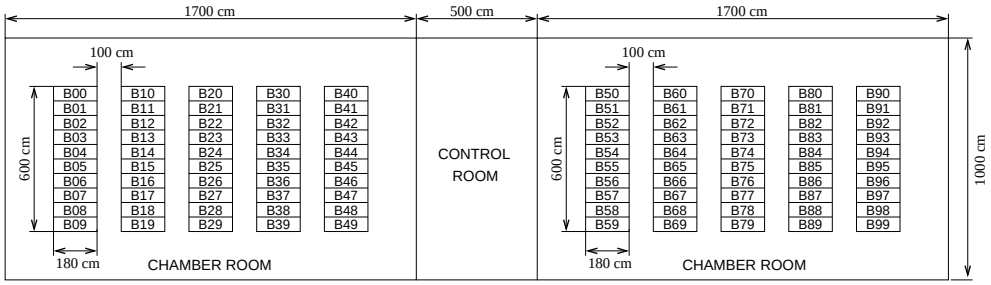


**Fig. 1.** Arrangement of 100 burst detectors set up in two rooms. The area of each burst detector is 50 cm $\times$ 160 cm and four emulsion chambers are set up on each burst detector.

Within the ground-based air shower experiments, those set up at higher altitudes are preferable for the physics studies at the knee region as discussed elsewhere. With these advantages, we carried out a hybrid experiment of emulsion chamber, burst detector and air shower array at Yangbajing (4300 m above sea level) in Tibet during the period from 1996 through 1999 (Amenomori et al., 2000a ; Amenomori et al., 2000b). Using the observed burst events (high-energy air shower cores) accompanying air showers with energies at the knee region, we obtained the primary energy spectra of protons and helium in the energy ranging from $2\times10^{14}$ eV to $10^{15}$ eV (Amenomori et al., 2000a) and the experiment suggests that almost all behavior of the observed burst events are compatible with the heavily enriched primary composition at the knee region (Amenomori et al., 2000b). Here, we report our further study on the flux of heavy component in the energy region beyond the knee.

## 2 Experiment

The Tibet-II air-shower array used in this experiment was comprised of 221 scintillation counters of 0.5 $m^2$ each of which were placed on a 15 m square grid, and observed air showers generated by primary particles in excess of about $10^{14}$ eV with an angular resolution better than 1°.

The burst detectors and ECs were used to detect high-energy air-shower cores accompanied by air showers. Each burst detector consisted of a plastic scintillator with the size of 160 cm $\times$ 50 cm and the thickness of 2 cm, and four photodiodes (PDs) were attached at four corners of each scintillator to read light signals generated by shower particles produced in the detector. Using the analog-to-digital converter (ADC) values from four PDs the total number (i.e., burst size, $N_b$, for each burst detector) and the position of the number-weighted center of all shower particles that hit a burst detector can be estimated (Amenomori et al., 2000a). The burst size capable of measuring with each detector ranges from $10^4$ to $3\times10^6$, roughly corresponding to shower energies raing-ing from ∼2 to ∼300 TeV. One hundred burst detectors (the whole area is 80 $m^2$) were separately set up in two rooms (it is by halves respectively), as shown in Fig.1. The emulsion chambers each having the size of 40 cm $\times$ 50 cm and the thickness 15 r.l. (lead plates) were put just above the burst detectors. The result obtained from the emulsion chambers will be reported elsewhere.

A burst event was triggered when any twofold coincidence of signals from four PDs of a burst detector appeared. Using the burst detector array, the electromagnetic components in the air-shower cores can be measured in the area within a radius of several meters. The coincidence of a burst event and an air-shower event was made by comparing their arrival times.

## 3 Data analysis and simulation

The data set of the burst events analyzed in this paper was taken from 16 October 1996 to 1st June 1999. We scanned the target maps of all events by the naked eye firstly. All those events showing a systematic noise configuration were ruled out during the first scanning (Amenomori et al., 2000b). Then we removed the events which are not coincident with the air shower events recorded by the Tibet-II air shower array.

In order to remove the showers generated by light nuclei, such as protons and helium nuclei, as much as possible, we first imposed the following conditions to the events: (1) number of fired detectors ($N_{bd}$) with the burst size $N_b \geq 3\times10^4$ is larger than 10; (2) air shower size $N_e$ should be larger than $10^{6.5}$. (3) zenith angle $\theta \leq 25°$ ($\sec\theta \leq 1.1$). Here, the minimum burst size is set to $3\times10^4$ in order to remove the influence of background noise. From this procedure, we selected 51 events in total.

An extensive Monte Carlo simulation was carried out to simulate the cascade developments of incident cosmic rays in the atmosphere and the burst detector responses. We used the CORSIKA+QGSJET code (Heck, 1998) to generate air shower events in the atmosphere. A heavy dominant (HD) model (Amenomori et al., 2000a) was adopted as an input primary spectrum in the present simulation. All shower particles were followed till 10 GeV by a full Monte Carlo method and then till 0.5 GeV by the thinning algorithm. An EPICS code (Kasahara, 1998) was used to simulate electromagnetic cascade showers in the ECs and burst detector. Cascade developments of secondary particles with energy above 0.5 GeV

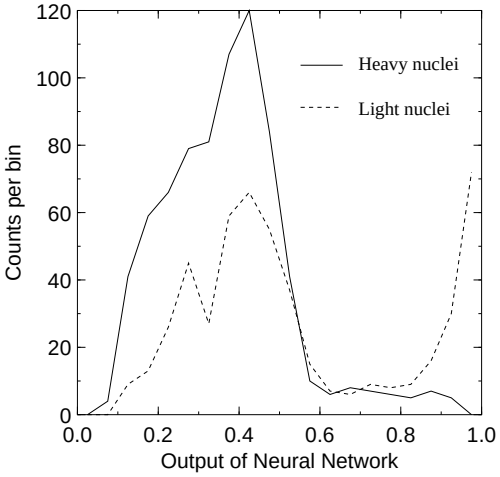


**Fig. 2.** ANN output distribution of the CORSIKA+HD simulation events. The solid and dashed lines denote the heavy nuclei and the light nuclei, respectively.

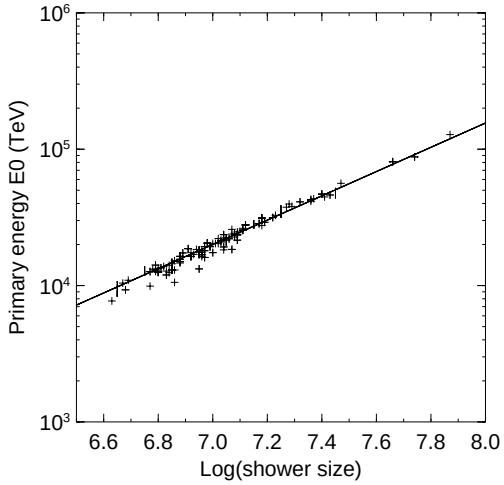


**Fig. 3.** Scatter plots between the primary energy $E_0$ versus air shower size $N_e$. for the events induced by heavy nuclei after the ANN selection (output value = 0.21).

in the detector were calculated analytically and then burst size just below the lead plate was obtained. Fluctuations of the number of cascade particles in the detector were adequately taken into account.

Using the same selection criteria as used in the experiment, we obtained 3538 simulation events in which the heavy components ($H$, $VH$, and Fe) are found to be about 56% (when a heavy dominant primary is assumed). Each event can be characterized by the following seven parameters: (1) $\sum N_b/Ne$; (2) mean lateral spread: $\langle \mathrm{R} \rangle = \sum N_b^i \times r_i / \sum N_b^i$, where $N_b^i$ and $r_i$ are the burst size of i-th detector and its distance from the top-detector; (3) $\langle N_b \rangle / \langle \mathrm{R} \rangle$; (4) $\langle N_b^i \times r_i \rangle$; (5) spread of energy flow: $R_{90}$, where 90% of the total energy flow is contained within the circle of a radius $R_{90}$. (6) $N_b^{top}/N_b^{half}$; where $N_b^{half}$ is the burst size of the top to $(N_{bd}/2)$th-detector ( when $N_{bd}$ is odd number, we use $N_{db}$-1 instead of $N_{bd}$). (7) $R^{half}$, which is the distance between the top-detector and the top to $(N_{bd}/2)$th-detector. In general, the events induced by heavy primaries may be characterized by bigger values of the parameters (2), (4), (5), and (7) and by smaller values of the parameters (1), (3), and (6), while those induced by light nuclei may have the opposite characters.

## 4 Results

In the previous paper (Amenomori et al., 2000a), we showed that a feed forward artificial neural network (ANN) is very effective in separating the proton-induced events from others. Here we also used a three-layered feed forward ANN as classifier of the species of primary particles with one hidden layer. The ANN we used has 7 and 15 neurons in input and hidden layer, respectively and 1 neuron for output layer. We trained and tested the ANN using the simulation events by dividing them into two groups, one is training dataset, the other is test dataset. The target value for heavy components($H$, $VH$, and Fe) is put 0 and for light nuclei (P, He, and CNO) to 1.

Using the simulation data mentioned above and a strict middle-point condition (Amenomori et al., 2000a), the classification ability of the network was checked by examining the fraction of the correct classification as a function of the number of epochs of the weight updating. The ANN output distribution of the test events is presented in Fig. 2. As seen in this figure, separation of heavy nuclei and others is not so good compared to that for protons (Amenomori et al., 2000a). In this experiment, since the performance of the burst detector is designed so that it may become advantageous to observation of proton-induced events (minimum burst size to be detected is very high, i.e., $3\times10^4$), separation of Fe and CNO events is considered to become bad. This bias becomes larger for events in lower energy region, in other words, this will bring a result which detects an event with the sharp core preferentiallly. Hence, the events accompanied by shower size corresponding to primary energy higher than $10^{16}$ eV or more were sorted out in the first analysis. Then, we obtained 11 heavy-induced events by setting ANN output cut to 0.21, and the fraction of correct classification was estimated to be about 80%.

The primary energy of each event can be estimated from shower size observed with the Tibet-II array. Shown in Fig. 3 is the scatter plots between the shower size $Ne$ and the primary energy $E_0$ for the events induced by heavy nuclei which were selected from the dataset of the simulation events by setting the ANN output value to 0.21. A fairly good correlation between $E_0$ and $Ne$ enables us to estimate the primary energies of observed burst events with small ambiguity.

Figure 4 shows the effective collecting area of the burst array calculated for primary heavy nuclei incident at the top of the atmosphere isotropically within the zenith angle smaller

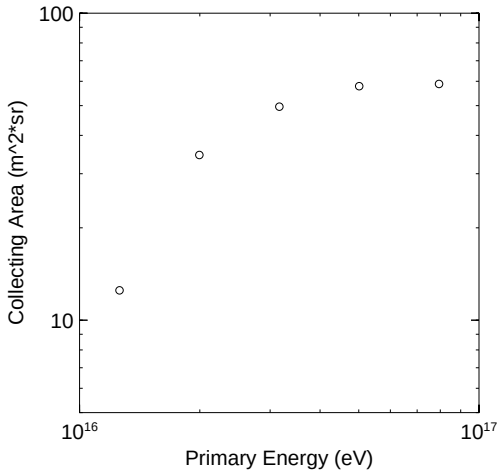


**Fig. 4.** Effective collecting area of the burst array for heavy component.

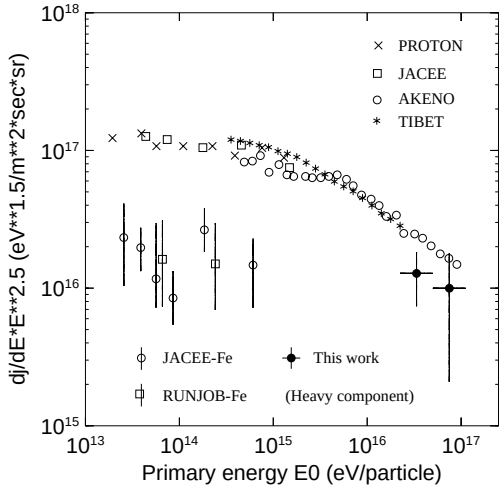


**Fig. 5.** Energy spectrum of primary heavy component ($H$, $VH$, and Fe). Iron flux data are from JACEE and RUNJOB. All-particle primary spectrum is taken from the Tibet experiment, AKENO and direct observations of Proton Satellite, JACEE. For details of the all-particle spectrum, see the paper (Amenomori et al., 2000a).

than $25^\circ$. The burst events satisfying the above selection criteria and accompanying air showers with $N_e \geq 10^{6.5}$ are selected in this calculation.

We show the result on the flux of heavy component ($H$, $VH$, and Fe) obtained from this experiment in Fig. 5, where direct measurements of iron component in lower energy region by JACEE (Asakimori et al., 1998) and RUNJOB (Apanashenko et al., 2001) are also presented for comparison. Our result suggests that the heavy component becomes very superior at energies around $10^{16}$-$10^{17}$ eV. This result will be further confirmed by a new experiment which is planned to be done at Yangbajing in the very near future.

## 5 Summary

We had successfully operated a hybrid experiment of the burst detector, emulsion chamber, and Tibet-II air-shower array during the period from 1996 through 1999. Using the data obtained with the burst detector and the air-shower array, and applying a neural network analysis to this data set, we obtained the absolute flux of primary heavy component in the energy region between $10^{16}$ eV and $10^{17}$ eV. Our data are compatible with the heavy enriched composition in the energy region beyond the knee.

*Acknowledgements.* This work is supported in part by Grants-Aid for Scientific Research and also for International Scientific Research from the Ministry of Education, Culture, Sports, Science and Technology in Japan and the Committee of Natural Science Foundation and Academy of Sciences in China.

## References

Amenomori, M. et al., Phys. Rev. D 62, 112002, 2000a.
Amenomori, M. et al., Phys. Rev. D 62, 072007, 2000b.
Apanashenko, A.V. et al., Astropart. Phys., in press, 2001.
Asakimori, K. et al., ApJ, 502, 278, 1998.
Heck, D. et al., Forschungszentrum Karlsruhe Report No. FZKA 6019, 1998.
Kasahara, K., http://eweb.b6.kanagawa-u.ac.jp/~kasahara/ ResearchHome/EPICSHome/index.html